

<https://helda.helsinki.fi>

---

## The first known virus isolates from Antarctic sea ice have complex infection patterns

Luhtanen, Anne-Mari

2018-04

---

Luhtanen , A-M , Eronen-Rasimus , E L , Oksanen , H M , Tison , J-L , Delille , B , Dieckmann , G S , Rintala , J-M & Bamford , D H 2018 , ' The first known virus isolates from Antarctic sea ice have complex infection patterns ' , FEMS Microbiology Ecology , vol. 94 , no. 4 , 028 . <https://doi.org/10.1093/femsec/fiy028>

---

<http://hdl.handle.net/10138/300595>  
<https://doi.org/10.1093/femsec/fiy028>

---

acceptedVersion

---

*Downloaded from Helda, University of Helsinki institutional repository.*

*This is an electronic reprint of the original article.*

*This reprint may differ from the original in pagination and typographic detail.*

*Please cite the original version.*

1  
2  
3 **1 Host specificity and temperature adaptation of the first known Antarctic sea-**  
4 **2 ice virus isolates**  
5  
6  
7 **3**

8 Anne-Mari Luhtanen<sup>1,2,3</sup>, Eeva Eronen-Rasimus<sup>1</sup>, Hanna M. Oksanen<sup>2</sup>, Jean-Louis  
9 Tison<sup>4</sup>, Bruno Delille<sup>5</sup>, Gerhard S. Dieckmann<sup>6</sup>, Janne-Markus Rintala<sup>3,7</sup> and  
10 Dennis H. Bamford<sup>2</sup>  
11  
12  
13  
14  
15

16 <sup>1</sup>Marine Research Centre, Finnish Environment Institute, Helsinki, Finland,  
17

18 <sup>2</sup>Programme on molecules, cells and systems, University of Helsinki, Helsinki,  
19 Finland, <sup>3</sup>Tvärminne Zoological Station, University of Helsinki, Hanko, Finland,  
20

21 <sup>4</sup>Laboratoire de Glaciologie, DGES, Université Libre de Bruxelles, Belgium,  
22

23 <sup>5</sup>Unité d'Océanographie Chimique, Université de Liège, Belgium, <sup>6</sup>Alfred  
24 Wegener Institute Helmholtz Center for Polar and Marine Research, Bremerhaven,  
25 Germany, <sup>7</sup>Department of Environmental Sciences, University of Helsinki,  
26 Helsinki, Finland  
27  
28  
29  
30

31  
32  
33  
34  
35 Correspondence:  
36

37 D.H. Bamford, Programme on molecules, cells and systems, FIN-00014 University  
38 of Helsinki, Finland. E-mail: dennis.bamford@helsinki.fi  
39  
40  
41

42 **22 Conflict of Interest**  
43

44 The authors declare no conflict of interest.  
45  
46  
47  
48  
49  
50  
51  
52  
53  
54  
55  
56  
57  
58  
59  
60

1  
2  
3 26 **Abstract**

4 27 Viruses are recognized as important actors in ocean ecology and biogeochemical  
5 28 cycles, but many details are not yet understood. We participated in a winter  
6 29 expedition to the Weddell Sea, Antarctica, to isolate viruses and to measure virus-  
7 30 like particle abundance (flow cytometry) in sea ice. We isolated 59 bacterial strains  
8 31 and the first four Antarctic sea-ice viruses known (PANV1, PANV2, OANV1, and  
9 32 OANV2), which grow in bacterial hosts belonging to the typical sea-ice genera  
10 33 *Paraglaciecola* and *Octadecabacter*. The viruses were cold-active and specific for  
11 34 bacteria at the strain level, although OANV1 was able to infect strains from two  
12 35 different classes. Both PANV1 and PANV2 infected 11/15 isolated *Paraglaciecola*  
13 36 strains that had almost identical 16S rRNA gene sequences, but the plating  
14 37 efficiencies differed among the strains, whereas OANV1 infected 3/7  
15 38 *Octadecabacter* and 1/15 *Paraglaciecola* strains and OANV2 1/7 *Octadecabacter*  
16 39 strains. The results showed that virus-host interactions can be very complex and  
17 40 that the viral community can also be dynamic in the winter-sea ice.  
18  
19  
20  
21  
22  
23  
24  
25  
26  
27  
28  
29  
30  
31  
32  
33  
34  
35  
36  
37  
38  
39  
40  
41

## 42 Introduction

43

44 Almost 10% of the world's ocean is covered by sea ice at least once per year,  
45 which makes it one of the largest biomes on Earth (Dieckmann and Hellmer 2010).

46 Although being a cold and harsh environment, sea ice is full of life. Specialized  
47 organisms live inside brine channels and pockets that are formed during freezing  
48 conditions, when salts and nutrients from the seawater become concentrated  
49 between the ice crystals (Thomas and Dieckmann 2002). The sea-ice microbial  
50 community consists of protists, bacteria, archaea, and their viruses (Maranger *et al.*  
51 1994; Mock and Thomas 2005; Arrigo *et al.* 2010; Deming and Collins 2017).

52 Here, we use the term bacteria instead of prokaryotes, even if in some cases  
53 archaea may also be involved. Microbes affect the biogeochemical properties of  
54 the sea ice, gas exchange between the ocean and atmosphere, and provide food for  
55 ice-associated animals, e.g. krill (Arrigo and Thomas 2004).

56

57 Viruses are the most numerous of life forms and are presumed to play important  
58 roles in the biogeochemical cycles of the oceans (Fuhrman 1999; Suttle 2007). The  
59 most commonly found viruses, bacteriophages (phages) i.e. viruses infecting  
60 bacteria, are possibly the main cause of bacterial mortality (Weinbauer 2004;  
61 Suttle 2007). Since viruses can multiply only within their host cells, their activity  
62 is dependent on the abundance and activity of their hosts (Maranger *et al.* 1994;  
63 Marchant *et al.* 2000). Due to their host specificity, they are crucial to control of  
64 bacterial community composition and activity (Proctor and Fuhrman 1990;  
65 Wommack and Colwell 2000; Suttle 2005; 2007). However, most studies of  
66 marine environments are conducted in the water column, whereas knowledge of  
67 viruses and their functions in sea ice is still very limited.

68

69 The numbers of virus-like particles (VLPs) measured, range between  $10^5$  and  $10^8$   
70  $\text{ml}^{-1}$  in bulk Arctic and Antarctic sea ice from spring to autumn. The lowest values

1  
2  
3 71 have been observed during the winter in Antarctic bulk ice (Paterson and  
4  
5 72 Laybourn-Parry 2012), whereas the highest numbers of VLPs occur during  
6  
7 73 freezing or spring algal mass growth (Maranger *et al.* 1994; Collins and Deming  
8  
9 74 2011). However, VLPs may also contain particles other than viruses, e.g. gene  
10  
11 75 transfer agents or membrane vesicles (Forterre *et al.* 2013; Soler *et al.* 2015). VLPs  
12  
13 76 are positively correlated with bacterial abundance, activity, and chlorophyll-*a* (chl-  
14  
15 77 *a*) concentrations (Maranger *et al.* 1994; Gowing *et al.* 2002, 2004). In aquatic  
16  
17 78 environments, a typical virus-to-bacteria ratio (VBR; more precisely VLP-to-  
18  
19 79 prokaryotic cell ratio) is 10:1 (Maranger and Bird 1995). Bacterial and viral  
20  
21 80 density specifies their contact rate, which is one of the key controls in virus-host  
22  
23 81 interactions. The semienclosed environment of brine channels may increase this  
24  
25 82 contact rate, especially during winter, when the brine channels are narrower and  
26  
27 83 the brine even more concentrated (Wells and Deming 2006a). Sea ice may,  
28  
29 84 therefore, be a place where virus-host interactions can be enhanced, compared with  
30  
31 85 the open ocean. To understand these effects, virus-host systems need to be isolated  
32  
33 86 to examine their interactions in detail.

34  
35 87

36  
37 88 To the best of our knowledge, only three virus-host systems to date have been  
38  
39 89 isolated from Arctic and seven from Baltic sea ice (Borriss *et al.* 2003; Luhtanen *et*  
40  
41 90 *al.* 2014, Yu *et al.* 2015), but none from Antarctic sea ice. The viruses isolated  
42  
43 91 represented different phage morphologies. The Arctic virus isolates *Shewanella*  
44  
45 92 phage 1a and *Colwellia* phage 21c are icosahedral viruses with either a contractile  
46  
47 93 or noncontractile tail, resembling double-stranded DNA (dsDNA) phages of the  
48  
49 94 order *Caudovirales* (Borriss *et al.* 2003; 2007). The filamentous nonlytic phage  
50  
51 95 f327 from the Arctic infects a *Pseudoalteromonas* strain and is reminiscent of  
52  
53 96 viruses in the family *Inoviridae* (Yu *et al.* 2015). In addition, seven tailed  
54  
55 97 icosahedral dsDNA phages infecting strains from either *Flavobacterium* or  
56  
57 98 *Shewanella* were isolated from Baltic Sea ice (Luhtanen *et al.* 2014; Senčilo *et al.*  
58  
59 99 2015). All virulent sea-ice phage isolates have a narrow host range, are cold-active

1  
2  
3 100 (capable of infection and production at  $\leq 4$  °C; Wells and Deming 2006b), and  
4  
5 101 produce plaques (clear zones on bacterial lawns used to determine the number of  
6  
7 102 infectious viruses) only at the lower end of their host bacterial temperature growth  
8  
9 103 range (Borriss *et al.* 2003; Luhtanen *et al.* 2014). In addition, a cold-active  
10  
11 104 siphophage 9A was isolated from Arctic nepheloid layer seawater (Wells and  
12  
13 105 Deming 2006b) for *Colwellia psychrerythraea* strain 34H, isolated originally from  
14  
15 106 Arctic shelf sediments (Huston *et al.* 2000). It was reminiscent of the isolates from  
16  
17 107 sea ice, because it also has a narrow host range, is cold-active, and has a more  
18  
19 108 restricted growth temperature range than the host bacteria.

20 109  
21  
22 110 Here, we report the isolation of the first cultivable phage-host systems and VLP  
23  
24 111 abundance from the winter-sea ice in the Weddell Sea, Antarctica. Studying phage-  
25  
26 112 host systems gives us valuable information on sea-ice microbial communities and  
27  
28 113 their potential roles in the sea-ice ecosystem.

29 114  
30  
31  
32  
33  
34  
35  
36  
37  
38  
39  
40  
41  
42  
43  
44  
45  
46  
47  
48  
49  
50  
51  
52  
53  
54  
55  
56  
57  
58  
59  
60

## 115 **Materials and Methods**

### 116 **Sea-ice sampling and ice properties**

117 Pack ice samples were collected from the Weddell Sea (Antarctica) during the  
118 austral winter as part of the Antarctic Winter Ecosystem Climate Study (AWECS)  
119 aboard R/V Polarstern in June–August 2013 (leg ANT-XXIX/6). Sampling was  
120 performed either with a metal basket (pancake ice at stations 486, 488, and 489) or  
121 using a motorized, trace-metal-clean (electropolished steel) CRREL-type ice-  
122 coring auger (Lannuzel *et al.* 2006), 14 cm in diameter. For this study, full-depth  
123 ice cores (one or two) were taken from 10 locations (ice-stations 486, 488, 489,  
124 493, 496, 500, 503, 506, 515, and 517) (Table 1), as described in Tison *et al.* 2017.  
125 Bulk ice was used, because some of the microbes may have been attached to the  
126 brine channel walls and could have been lost if only the liquid brine were sampled  
127 (Meiners *et al.* 2008). The ice cores were cut into one, three, five, or seven layers,  
128 depending on the ice thickness, and crushed gently with a hammer inside a  
129 polyethylene plastic bag. The corresponding layers of the possible sibling ice cores  
130 were pooled (Table 1). The VLP abundances were measured from these layers.  
131 The bacterial abundances (Table 1), bacterial production (measured as thymidine  
132 incorporation), and bacterial community composition analyses from these ice cores  
133 have been published elsewhere (Eronen-Rasimus *et al.* 2017). For the isolation  
134 work, we used the ice samples from first-year ice-station 500 and early second-  
135 year ice-station 515a (Tison *et al.* 2017). The surface parts of the 515a core were  
136 removed to minimize contamination, and the core was cut into 12 layers (~14 cm  
137 each; Table 2), using an electric-band saw sterilized with 70% ethanol. The 12  
138 layers were used separately to isolate the bacterial strains. The bacterial  
139 community composition of ice core 515a has also been published under the name  
140 515 T (0–56 cm), M (56–126 cm), and B (126–166 cm) (Eronen-Rasimus *et al.*  
141 2017). For virus isolation, bulk ice from station 500 and core 515a was used. The  
142 ice samples were left to melt in sterilized containers at 4 °C overnight, after which

1  
2  
3 143 the remaining ice was melted in a water bath with continuous shaking (Rintala *et*  
4 *al.* 2014). After melting, the samples were immediately transferred back to 4 °C.

5 144  
6 145  
7  
8 146 The pancake ice at stations 486 and 488 was 6 cm and 35 cm thick, the first-year  
9  
10 147 ice at stations 489–506 and 517 was 37–90 cm, and the early second-year ice at  
11  
12 148 station 515 was 179 cm (Table 1, Tison *et al.* 2017). The ice temperature varied  
13  
14 149 between -1.7 and -12.6 °C, with a median temperature of -3.8 °C and ice *chl-a*  
15  
16 150 median concentration of 2.4 µg l<sup>-1</sup> (Tison *et al.* 2017). The ice at station 500 was  
17  
18 151 dominated by frazil ice and at station 515 by mixed columnar and frazil ice (Tison  
19  
20 152 *et al.* 2017). The brine salinity varied from 122 to 40 practical salinity units (Tison  
21  
22 153 *et al.* 2017).

### 23 154 24 25 155 **Isolation of the bacterial strains**

26  
27 156 Isolation of the bacterial strains was started immediately after the 12 layers of the  
28  
29 157 ice core 515a samples were melted. The strains were isolated by plating 100 µl of  
30  
31 158 the melted sample on (I) ZoBell plates (1000 ml Southern Ocean water, 5 g  
32  
33 159 peptone, 1 g yeast extract, 15 g agar; Helmke and Weyland 1995; Middelboe *et al.*  
34  
35 160 2003), (II) concentrated ZoBell plates (the Southern Ocean water was concentrated  
36  
37 161 by boiling to half of the initial volume, otherwise similar to ZoBell), and (III)  
38  
39 162 Modified Oxford (MOX) agar plates (750 ml seawater, 250 ml ultrapure water, 1 g  
40  
41 163 KNO<sub>4</sub>, 0.2 g yeast extract, 10 mg FePO<sub>4</sub>, 2 g HEPES, 12 g agar). The plates were  
42  
43 164 incubated at 4 °C and transported from R/V Polarstern to the home laboratory with  
44  
45 165 temperature-controlled courier transportation at -2.6 °C to +6.1 °C (World Courier,  
46  
47 166 AmerisourceBergen, Stamford, CT, USA). After 1 month of incubation in the dark  
48  
49 167 at 4 °C, the various colony morphotypes were picked and colony-purified at three  
50  
51 168 consecutive times. Colony purification and cultivation were done on modified  
52  
53 169 ZoBell medium, Reef Crystal (RC) medium: 33 g Reef Crystals, Aquarium  
54  
55 170 Systems Inc. Sarrebourg, France, 1000 ml ultrapure water, 5 g peptone, 1 g yeast  
56  
57 171 extract). The agar concentration for the plates was 1.5% (w/v). The strains were



1  
2  
3 172 grown aerobically in RC medium at 4 °C for 7 days and stored at -80 °C,  
4 173 supplemented with 15% (v/v) glycerol.

5  
6 174

### 7 8 175 **Identification of the bacterial strains**

9  
10 176 The colony-purified strains were identified by 16S rRNA gene sequencing. The  
11 177 genomic DNA was isolated with an UltraClean Microbial DNA Isolation Kit (MO  
12 178 BIO Laboratories Inc., Carlsbad, CA, USA). The partial 16S rRNA genes were  
13 179 amplified with PCR, using primers F27 (Sait *et al.* 2003) and R1406 (Lane *et al.*  
14 180 1985) or pA and pGr (Edwards *et al.* 1989). The Sanger sequencing was performed  
15 181 at the DNA Sequencing and Genomics Unit, Institute of Biotechnology (University  
16 182 of Helsinki), using primers pDr, pE, and pFr (Edwards *et al.* 1989). The taxonomic  
17 183 identification of the strains was done with SILVA Incremental Aligner (SINA)  
18 184 Alignment Service (version 1.2.11, 10.6.2016, Pruesse *et al.* 2012). The partial 16S  
19 185 rRNA gene sequences of the isolated bacterial strains are deposited in the NCBI  
20 186 GenBank database under accession numbers KY194799–KY194857 (Table 2).

21  
22 187

### 23 188 **Phylogenetic analysis of the 16S rRNA sequences**

24 189 For the phylogenetic tree, alignment was performed with SINA Alignment Service  
25 190 (version 1.2.11, minimum identity: 0.8, Pruesse *et al.* 2012). Reference sequences  
26 191 were selected, based on SINA sequence matching, and for the nontype-strain  
27 192 sequence matches, their type-strain representatives were also added (EZBioCloud  
28 193 Database (Yoon *et al.* 2017). The 16S rRNA sequence of *Sulfolobus tokodaii*  
29 194 (AB022438) was used as an outgroup in the alignment. After the alignment, all  
30 195 sequences were truncated according to the sequence length, and the bootstrapped  
31 196 (1000) maximum-likelihood tree was constructed, using RAxML (version 8.2.0;  
32 197 Stamatakis 2014), with the GTRGAMMA evolution model. The tree was  
33 198 visualized with the Interactive Tree Of Life (iTOL) online tool (Letunic and Bork  
34 199 2007).

35  
36 200

## 201 **Abundance of virus-like particles by flow cytometry**

202 The abundances of the VLPs were analyzed with flow cytometry from all the ice  
203 layers originating from the 10 stations (Table 1). Sample handling and  
204 measurements were done according to Brussaard *et al.* (2010), except that  
205 paraformaldehyde [1% (v/v) in phosphate-buffered saline (PBS), Alfa Aesar  
206 GmbH & Co KG, Karlsruhe, Germany] was used as a fixative. The samples were  
207 stained with SYBR Green I (Sigma-Aldrich Inc., Saint Louis, MO, USA) at room  
208 temperature. To measure the background, virus-sized particles were removed from  
209 the control samples by ultrafiltration (Amicon Ultra-15 concentrators, MWCO 100  
210 000 Da; Merck Millipore, Billerica, MA, USA; 4000 g, 4 min, 4 °C), and the  
211 controls were processed in the same way as the actual samples. Earlier isolated and  
212 purified 1/4, 1/32, 1/40, 1/41, 1/44, 3/49 phage particles (Luhtanen *et al.* 2014)  
213 were used as controls to define the virus population, and Fluoresbrite 0.5- $\mu$ m  
214 microspheres (Polysciences Inc., Warrington, PA, USA) were used as a size  
215 standard. Enumeration of the diluted samples (dilution factor 10; molecular  
216 biology grade TE buffer, AppliChem GmbH, Darmstadt, Germany) was carried  
217 out, using a CyFlow Cube 8 (Partec GmbH, Münster, Germany) flow cytometer  
218 equipped with a 488-nm laser. The data were analyzed, using FCS Express 4  
219 software (De Novo Software, Glendale, CA, USA), and the numbers were  
220 corrected for dilution. The VBR was defined, using the bacterial abundance results  
221 published earlier (Eronen-Rasimus *et al.* 2017).

222

## 223 **Isolation of viruses**

224 For virus isolations, the melted layers of the station 500 core were pooled, as were  
225 the layers of core 515a. The melted ice was filtered through a 0.22- $\mu$ m Durapore  
226 Membrane polyvinylidene difluoride (PVDF) filter (EMD Millipore Corporation,  
227 Billerica, MA, USA) to remove cellular organisms. The filtrates were concentrated  
228 50 times, using Amicon Ultra-15 concentrators (MWCO 100 000 Da) and  
229 centrifugation (2000 g, 5 min, 4 °C). The concentrates were stored in 15% (v/v)

1  
2  
3 230 glycerol at -80 °C and transported in liquid nitrogen to the home laboratory. All  
4  
5 231 isolated and colony-purified bacterial strains (Table 2, Figure 1) that were able to  
6  
7 232 form a bacterial lawn were used to isolate viruses. Virus isolation and further  
8  
9 233 cultivation were done with a plaque assay. For virus isolation, 10 µl and 100 µl of  
10  
11 234 the concentrated sample with 200 µl of dense host bacterial suspension (grown for  
12  
13 235 7 days in RC medium at 4 °C) and 3 ml of melted RC top-layer agar [0.4% (w/v)  
14  
15 236 agar; 43 °C] were mixed and poured on RC plates. After 1–3 weeks of incubation  
16  
17 237 at 4 °C, the plaques were individually picked and plaque-purified three consecutive  
18  
19 238 times with the plaque assay. For the plaque assay, 100 µl of suitable virus dilution,  
20  
21 239 200 µl of host liquid culture, and 3 ml of RC top-layer agar were mixed and poured  
22  
23 240 on RC plates, which were incubated for 5–7 days at 4 °C.  
24

241

#### 242 **Production and purification of viruses**

243 The virus lysates were prepared with the plaque assay as described above, using  
244 semiconfluent plates. The top-layer agar was collected and mixed with 2 ml of RC  
245 broth per plate. The suspension was incubated for 1 h at 4 °C with shaking, after  
246 which the cell debris and agar were removed (centrifugation: 10 000 g, 30 min, 4  
247 °C). Virus precipitation from the lysates was optimized with various ammonium  
248 sulfate concentrations [50%, 60%, 70%, and 80% (w/v)], using either saturated  
249 solution or ammonium sulfate powder (Boulanger and Puvion 1973; Burgess  
250 2009). Ammonium sulfate was mixed with or dissolved in the lysate for 1 h at 4 °C  
251 with shaking. The precipitated viruses were collected (centrifugation: 14 000 g, 60  
252 min), washed with SM buffer (50 mM Tris-HCl pH 7.5, 100 mM NaCl, 8 mM  
253 MgSO<sub>4</sub>; Borriss *et al.* 2003) with or without 0.01% (w/v) gelatin and dissolved in  
254 SM buffer on ice. The virus aggregates were removed (centrifugation 9300 g, 10  
255 min, 4 °C), and the viruses in the supernatant were subjected to rate-zonal  
256 centrifugation (153 208 g, 30–70 min, 10 °C), using 10–30% (w/v) linear sucrose  
257 gradients in SM buffer (Anderson *et al.* 1966; Lawrence and Steward 2010). The  
258 gradients were fractionated (12 fractions), and the infectivity (plaque assay),

1  
2  
3 259 absorbance (260 nm), and the protein, nucleic acid, and lipid contents of the  
4  
5 260 fractions were determined (see below). The virus particles in the light-scattering  
6  
7 261 zones were collected with differential centrifugation (104 087 g, 3 h, 10 °C), and  
8  
9 262 the particles were dissolved in SM buffer overnight on ice.

10  
11 263

### 12 264 **Virus particle analyses**

13  
14 265 The absorbance values (260 nm) of the 12 sucrose gradient fractions were  
15  
16 266 measured with an Eppendorf BioPhotometer D30 (Eppendorf AG, Hamburg,  
17  
18 267 Germany), using 30% (w/v) sucrose in SM buffer as a blank sample. The viral  
19  
20 268 structural proteins were separated with SDS-PAGE (16% (w/v) acrylamide;  
21  
22 269 Olkkonen and Bamford 1989). The SM buffer used in the protein analysis samples  
23  
24 270 did not contain gelatin. The protein concentrations were determined with a  
25  
26 271 Coomassie Blue-based method (Bradford 1976), using bovine serum albumin as a  
27  
28 272 standard. For the SDS-PAGE, when appropriate, the samples were concentrated  
29  
30 273 with 10% (v/v) trichloroacetic acid precipitation (30 min, on ice). The precipitate  
31  
32 274 was collected (centrifugation: 16 200 g, 30 min, 4° C). The resolving gels were  
33  
34 275 stained with Brilliant Blue R (Sigma-Aldrich) for proteins and, when appropriate,  
35  
36 276 stained with Sudan Black B (Sigma-Aldrich) for lipids and the stacking gels with  
37  
38 277 ethidium bromide for nucleic acids. For the lipid-staining control, purified PRD1  
39  
40 278 particles (Bamford and Bamford 1991) were used as a control. To test the  
41  
42 279 sensitivity of the viruses to Triton X-100, viruses were incubated in 0.1% (v/v) and  
43  
44 280 0.01% Triton X-100 (in SM buffer) for 3 h and 24 h at 4 °C. SM buffer was used  
45  
46 281 as a control. The infectivity of the viruses tested was determined with a plaque  
47  
48 282 assay. The sensitivity of the host organisms to Triton X-100 was analyzed  
49  
50 283 similarly, except that the number of colony-forming units was determined by  
51  
52 284 plating. For TEM, the purified virus particles were negatively stained for 20 s,  
53  
54 285 using 2% (w/v) uranyl acetate (pH 7), 3% (w/v) uranyl acetate (pH 4.5), or 1%  
55  
56 286 potassium phosphotungstate (pH 7). A JEOL JEM-1400 TEM (Electron

1  
2  
3 287 Microscopy Unit, Institute of Biotechnology, University of Helsinki) was used  
4 288 with 80-kV tension for detailed investigation of the viruses.

5  
6 289

7  
8 290 **Temperature ranges of host growth and virus infection**

9  
10 291 The growth of the original three host strains at different temperatures was  
11  
12 292 determined by plating 100 µl of diluted bacterial suspension on RC plates, which  
13  
14 293 were incubated at 0, 4, 10, 15, or 20 °C for 60 days. The infection ability of the  
15  
16 294 bacteriophages at different temperatures was tested with a plaque assay. The host  
17  
18 295 suspensions used for the plaque assay were incubated at 4 °C. The plates were  
19  
20 296 incubated at 0, 4, 10, or 15 °C for 20 days.

21  
22 297

23  
24 298 **Virus-prokaryote interactions**

25 299 All the bacterial isolates that were able to grow as a lawn on a plate were tested for  
26  
27 300 their sensitivity to the isolated viruses (Table 2, Figure 1). Ten microliters of  
28  
29 301 undiluted and 100-times diluted virus lysates were spotted on the host strain lawns.  
30  
31 302 RC medium was used as a negative control and the original virus-host pair as a  
32  
33 303 positive control. The plates were incubated at 4 °C for 7–14 days. All positive  
34  
35 304 results were verified with a plaque assay, using suitable dilutions of the virus. The  
36  
37 305 EOP was calculated according to the plaque count obtained with the target strain,  
38  
39 306 compared with that obtained with the isolation host strain.

40  
41 307  
42  
43  
44  
45  
46  
47  
48  
49  
50  
51  
52  
53  
54  
55  
56  
57  
58  
59  
60

## 308 **Results**

### 309 **Sea-ice bacterial isolates**

310 We isolated 59 bacterial strains from core 515a (Table 2). The majority of the  
311 isolates (~59%) were classified as members of the genera *Glaciececola* or  
312 *Paraglaciecola* (Figure 1). Only one strain, IceBac 363, was isolated from the  
313 coldest top layer and belonged to the genus *Halomonas*. The remaining strains  
314 were identified as members of the genera *Octadecabacter* (seven strains),  
315 *Polaribacter* (seven strains), *Marinobacter* (three strains), *Pseudoalteromonas*  
316 (three strains), *Colwellia* (two strains), or *Paracoccus* (one strain). All isolated  
317 bacterial strains belonging to the same genus had identical or nearly identical  
318 (identity 99.3–100%) partial 16S rRNA gene sequences (at minimum 1290 base  
319 pairs, bp).

320

### 321 **Virus-like particle abundance and virus-to-bacteria ratios in sea ice**

322 The mean VLP abundance was  $1.1 \times 10^6 \text{ ml}^{-1}$  (range  $1.9 \times 10^5$ – $4.9 \times 10^6 \text{ ml}^{-1}$ ) in the  
323 bulk ice, with the highest numbers at stations 500 and 515 ( $0.7 \times 10^6$ – $4.9 \times 10^6 \text{ ml}^{-1}$ ;  
324 Table 1). The mean VBR was 5.3 (range 0.7–13.4; Table 1). The highest VBR  
325 values were at station 503 (9.5–13.4; Table 1) and the lowest at station 515 (0.7–  
326 2.9; Table 1).

327

### 328 **Sea-ice bacteriophage isolates**

329 Forty-eight out of the 59 bacterial strains were able to form a bacterial lawn on a  
330 plate and were consequently used to screen phages (Table 2). Four phages were  
331 obtained, cultivated, and purified in the laboratory (Table 3). The phages were  
332 named after the isolation host genus, area of isolation, and the initials of notable  
333 persons in this study (Krupovic *et al.* 2016). The names and their abbreviations are  
334 *Paraglaciecola* Antarctic GD virus 1 (PANV1), *Paraglaciecola* Antarctic JLT  
335 virus 2 (PANV2), *Octadecabacter* Antarctic BD virus 1 (OANV1), and  
336 *Octadecabacter* Antarctic DB virus 2 (OANV2). Phages PANV1 and PANV2

1  
2  
3 337 originated from station 500 and were isolated for the same host (IceBac 372),  
4 338 which was classified as *Paraglaciecola psychrophila* (similarity 99.9%). PANV1  
5 339 produced clear plaques 3–4 mm in diameter, whereas the PANV2 plaques of 3–5  
6 340 mm in diameter had a clear center surrounded by a turbid halo. Phages OANV1  
7 341 and OANV2 were isolated from core 515a for two different bacterial hosts, IceBac  
8 342 419 and IceBac 430, respectively, both identified as *Octadecabacter antarcticus*.  
9 343 Both phages produced clear plaques, but the diameters were different (3–6 mm for  
10 344 OANV1, 6–8 mm for OANV2). The optimized phage lysate titers varied from  
11 345  $\sim 6 \times 10^9$  to  $\sim 5 \times 10^{11}$  plaque-forming units (pfu) ml<sup>-1</sup>, depending on the phage (Table  
12 346 3). The infectivity of the lysates was retained for several months when stored at 4  
13 347 °C. All three host strains originated from different layers in the ice core (Table 2).  
14  
15  
16  
17  
18  
19  
20  
21  
22  
23  
24

### 25 349 **Purification and characterization of the phages**

26 350 To characterize the phages, virus purification methods were optimized, based on  
27 351 ammonium sulfate precipitation and rate-zonal ultracentrifugation, following the  
28 352 recovery and purity of the infectious viruses at each step. Using ammonium sulfate  
29 353 precipitation, 25–54% of the infectious viruses were recovered, depending on the  
30 354 virus (Table 4). Both the ammonium sulfate powder and the saturated solution  
31 355 resulted in similar yields. PANV1 and PANV2 were precipitated with 50%  
32 356 ammonium sulfate, whereas OANV1 and OANV2 needed 80%. The precipitated  
33 357 particles were further purified with rate-zonal ultracentrifugation, and significant  
34 358 amounts of various noninfectious protein impurity species were detected at the top  
35 359 of the sucrose gradient. For all viruses, a single visible infectious light-scattering  
36 360 zone was detected in the middle of the sucrose gradient (Figure 2). This zone  
37 361 contained several proteins of different sizes that were unique for each virus.  
38 362 PANV1 and OANV2 had one major protein type in sizes of  $\sim 55$  and  $\sim 35$  kDa,  
39 363 respectively, while PANV2 and OANV1 had two major protein types ( $\sim 40$  and  
40 364  $\sim 12$  kDa in PANV2;  $\sim 35$  and  $\sim 15$  kDa in OANV1). A peak in the absorbance was  
41 365 detected in the same light-scattering zone, as were the nucleic acids when visible.  
42  
43  
44  
45  
46  
47  
48  
49  
50  
51  
52  
53  
54  
55  
56  
57  
58  
59  
60

1  
2  
3 366 Lipids could not be detected from the gels after Sudan Black staining (not shown).  
4  
5 367 In addition, treatment of phages with the nonionic detergent Triton X-100 did not  
6  
7 368 affect their infectivity, suggesting that the virus particles did not contain a lipid  
8  
9 369 component. Specific infectivities ( $\sim 2 \times 10^{12}$  pfu mg<sup>-1</sup> protein) calculated for the  
10  
11 370 purified phages showed that all virus samples were highly infectious after  
12  
13 371 biochemical purification (Table 4). After the final concentration step with  
14  
15 372 differential centrifugation, the recoveries of infectious viruses varied from ~10% to  
16  
17 373 20% (Table 4).  
18

19  
20 375 Transmission electron microscopy (TEM) of the purified particles (Figure 3)  
21  
22 376 showed that phage PANV1 had a rigid, contractile tail typical of myoviruses. Its  
23  
24 377 average tail length was ~58 nm and head diameter ~71 nm. PANV2 infecting the  
25  
26 378 same host had an ~89-nm noncontractile tail characteristic of the siphoviruses and  
27  
28 379 an ~52-nm head diameter (Table 3). OANV1 also had a typical siphovirus tail,  
29  
30 380 with an average length of ~83 nm and a head ~50 nm in diameter, whereas  
31  
32 381 OANV2 seemed to have a very short tail typical of podoviruses and a head ~53 nm  
33  
34 382 in diameter (Table 3).  
35

### 36 384 **Temperature range tests for host growth and phage infection**

37  
38 385 All the bacterial host strains (IceBac 372, IceBac 419, and IceBac 430) were able  
39  
40 386 to form colonies at the temperatures from 0 °C to 15 °C, but not at 20 °C (Table 5),  
41  
42 387 and were therefore classified as psychrophiles (Morita 1975). The effect of  
43  
44 388 temperature on phage infection (plaque formation) was tested at temperatures  
45  
46 389 supporting the growth of the hosts. All the phages were able to infect their original  
47  
48 390 host only at 0 °C and 4 °C, but not at higher temperatures (Table 5). PANV1 and  
49  
50 391 PANV2 produced plaques at 0 °C and 4 °C in 6 days, but OANV1 and OANV2  
51  
52 392 produced plaques at 0 °C in 14 days and at 4 °C in 6 days.  
53

54 393

### 55 394 **Phage-bacteria interactions**



1  
2  
3 395 The sensitivity of all the 48 isolated bacterial strains (that were able to grow as a  
4 bacterial lawn) to the isolated phages was tested (Table 2; Figure 1). In all, 17  
5 396  
6 397 strains (13 *Paraglaciecola* strains and 4 *Octadecabacter* strains) were sensitive to  
7  
8 398 at least one of the phages (Figure 1). Of 16 *Paraglaciecola* isolates, IceBac 372  
9  
10 399 was sensitive to three phages: PANV1, PANV2, and OANV1. Ten other  
11  
12 400 *Paraglaciecola* strains were sensitive to both PANV1 and PANV2, but with  
13  
14 401 different plating efficiencies (EOPs), two strains were sensitive to either PANV1  
15  
16 402 or PANV2, but with low EOP, and three strains could not be infected. All seven  
17  
18 403 *Octadecabacter* strains had 100% identical 16S rRNA gene sequences (within  
19  
20 404 1289 bp, Figure 1). However, only four out of seven *Octadecabacter* strains were  
21  
22 405 sensitive to either OANV1 or OANV2 and showed different EOPs.  
23  
24 406

25 407 Both the PANV1 and PANV2 phages were able to infect 12 different  
26  
27 408 *Paraglaciecola* strains with different EOPs. However, each of them infected only a  
28  
29 409 certain strain (IceBac 417 or IceBac 420, respectively) that the other could not  
30  
31 410 (Figure 1). In addition to its original host strain (IceBac 419, *Octadecabacter*),  
32  
33 411 OANV1 was able to infect two other *Octadecabacter* strains, but with lower EOP.  
34  
35 412 It also produced plaques with high EOP in the strain IceBac 372 (*Paraglaciecola*),  
36  
37 413 which was the isolation host for PANV1 and PANV2 (Figure 1). Consequently,  
38  
39 414 OANV1 was able to infect strains representing two classes: Gammaproteobacteria  
40  
41 415 (*Paraglaciecola*) and Alphaproteobacteria (*Octadecabacter*). In contrast, phage  
42  
43 416 OANV2 was able to infect only IceBac 430 (*Octadecabacter*; Figure 1).  
44  
45 417

## 418 Discussion

419

420 We isolated and purified four Antarctic sea-ice phages (PANV1, PANV2,  
421 OANV1, and OANV2) that could be maintained and cultivated under laboratory  
422 conditions. They were cold-active (capable of infection and production at  $\leq 4$  °C;  
423 Wells and Deming 2006b), infecting bacterial strains belonging to the typical sea-  
424 ice bacterial genera *Paraglaciecola* or *Octadecabacter*. The viruses were specific  
425 for host recognition at the strain level, even though OANV1 was able to infect  
426 bacterial strains from two different classes. The highest VLP abundances were in  
427 the samples where bacteria were most abundant and active (Eronen-Rasimus *et al.*  
428 2017).

429

### 430 Isolation of sea-ice bacteria and phages

431 We isolated 59 bacterial strains belonging to nine different genera from Antarctic  
432 winter-sea ice. The ice was melted with the direct-melting method, which has been  
433 shown to result in viable bacteria counts similar to those obtained by melting with  
434 seawater addition (Helmke and Weyland 1995), even if it may cause osmotic stress  
435 due to the rapid salinity changes. The isolated strains belonged to the following  
436 genera: *Colwellia*, *Glaciecola*, *Halomonas*, *Marinobacter*, *Octadecabacter*,  
437 *Paracoccus*, *Paraglaciecola* (formerly *Glaciecola*; Shivaiji and Reddy 2014),  
438 *Polaribacter*, and *Pseudoalteromonas*, all of which are common members in the  
439 sea-ice bacterial community (Bowman *et al.* 1997; Brinkmeyer *et al.* 2003;  
440 Deming and Collins 2017). The majority of these genera were also abundant in  
441 isolation ice core 515a, based on bacterial community composition analysis (see  
442 results in Eronen-Rasimus *et al.* 2017).

443

444 In addition, four unique phages were isolated from the sea ice with the direct-  
445 melting and plaque assay methods, even though the viruses were exposed to a 43  
446 °C temperature for a short time during the plaque assay. This has also been

1  
2  
3 447 successfully used previously (Borriss *et al.* 2003), and at least some of the cold-  
4 448 adapted phages can apparently tolerate high temperatures for a short time. Wide  
5 449 temperature tolerance can be beneficial to phage survival in natural environments  
6  
7 450 throughout the various seasons.  
8  
9

10 451  
11  
12 452 Presumably, virus reproduction is most effective when the number of susceptible  
13 453 hosts is high and active (Thingstad and Lignell 1997). The hosts of the  
14 454 bacteriophages OANV1 and OANV2 belonged to the genus *Octadecabacter*,  
15  
16 455 which was abundant in phage isolation core 515a (Eronen-Rasimus *et al.* 2017).  
17  
18 456 The genus *Paraglaciecola* (host of phages PANV1 and PANV2) could not be  
19  
20 457 detected separately from the genus *Glaciecola* in the community analysis, likely  
21  
22 458 due to the short sequence length used, but *Glaciecola* was present in both the 500  
23  
24 459 and 515a cores (Eronen-Rasimus *et al.* 2017). Our results together with those of  
25  
26 460 Eronen-Rasimus *et al.* (2017) support the notion that bacteriophages of these  
27  
28 461 predominant bacteria may be abundant in the viral community, resulting in  
29  
30 462 increased opportunities of isolating them.  
31  
32

33 463

### 34 464 **Phage-host interactions**

35  
36 465 We tested the sensitivity of 48 isolated bacterial strains, representing nine different  
37  
38 466 genera, to our phages. PANV1 and PANV2 were able to infect several closely  
39  
40 467 related *Paraglaciecola* strains with different EOPs, but not all the strains (Figure  
41  
42 468 1). This may have been the result of an arms race in which bacterial strains evolve  
43  
44 469 to inhibit phage infection, leading to diversification of bacterial strains (Thingstad  
45  
46 470 *et al.* 2014). Since PANV1 and PANV2 infected different strains, this may have  
47  
48 471 resulted in two different phage-host coevolution lineages.  
49

50 472

51  
52 473 Phage OANV1 was able to infect bacterial strains from two different classes:

53  
54 474 Alphaproteobacteria (*Octadecabacter*) and Gammaproteobacteria (*Paraglaciecola*,  
55  
56 475 Figure 1). Still, it was able to infect only three of the *Octadecabacter* strains with  
57  
58  
59  
60

1  
2  
3 476 identical 16S rRNA gene sequences. These phages can seemingly be strain-  
4  
5 477 specific in their host recognition, even if they can infect bacteria across classes.  
6  
7 478 Sea-ice phage isolates have very narrow host ranges (Borriss *et al.* 2003; Luhtanen  
8  
9 479 *et al.* 2014), but based on the genomic data, cold-active phages may have broader  
10  
11 480 host ranges than mesophiles (Colangelo-Lillis and Deming 2013). Myoviruses are  
12  
13 481 often considered to have broader host ranges than siphoviruses and podoviruses  
14  
15 482 (Suttle 2005). However, in this study, myovirus PANV1 and siphovirus PANV2  
16  
17 483 showed similar host ranges and were able to infect only closely related hosts,  
18  
19 484 whereas siphovirus OANV1 was able to infect strains from two different classes.  
20  
21 485 When phage host ranges are experimentally studied, the number of cultivable  
22  
23 486 bacterial isolates limits the tests, and consequently the results cannot reveal the  
24  
25 487 complete host range spectrum in the environment. However, our results indicate  
26  
27 488 that with the strain specificity observed, the phages may be able to control the  
28  
29 489 bacterial community composition, as proposed earlier based on observation in the  
30  
31 490 environment (Maranger *et al.* 1994), theory (Thingstad *et al.* 2014), and  
32  
33 491 experimentation (Middelboe *et al.* 2001). Since viruses need their hosts to replicate  
34  
35 492 and produce progeny, their activity is directed to the active part of the bacterial  
36  
37 493 community.  
38

494

### 495 **Purification and characterization of phages**

496 The purification process was optimized for all phages separately. Purification  
497  
498 analysis revealed that a significant amount of impurities and host-derived  
499  
500 complexes were separated, allowing us to obtain a light-scattering zone comprising  
501  
502 infectious, highly purified viruses (Figure 2). The individual protein patterns of the  
503  
504 isolated phages (Figure 2) and the specific infectivities calculated (Table 4)  
505  
506 showed that each isolated phage was different and that the purification of the virus  
507  
508 particles was successful. Efficient purification made it possible to study individual  
509  
510 phages in more detail. Detailed TEM observations verified that all the phages  
511  
512 isolated were icosahedral tailed phages (Figure 3). Sudan Black staining of the

1  
2  
3 505 sodium dodecyl sulfate-polyacrylamide gel electrophoresis (SDS-PAGE) gel and  
4 506 Triton-X treatment of the virus particles indicated that the phages do not have a  
5 507 structural lipid component, which is in accordance with the virus morphologies  
6 508 observed. The virus capsid diameters (~50–71 nm; Table 3) are similar to those in  
7 509 the most abundant VLP size groups (50–70 nm or <110 nm) reported in Arctic and  
8 510 Antarctic sea ice (Maranger *et al.* 1994; Gowing *et al.* 2004). In three cases, the  
9 511 morphology of the virus tails was reliably identified, suggesting that PANV1 is a  
10 512 myovirus, whereas PANV2 and OANV1 are siphoviruses (Figure 3) resembling  
11 513 the dsDNA bacteriophages belonging to the order *Caudovirales*. However, the tail  
12 514 of bacteriophage OANV2 was considerably difficult to detect. We propose that  
13 515 OANV2 is a podophage with a short noncontractile tail. Icosahedral tailed viruses  
14 516 from the order *Caudovirales* were previously the most often isolated virus types  
15 517 from sea ice (Borriss *et al.* 2003; Luhtanen *et al.* 2014), although a filamentous  
16 518 virus from the order *Inoviridae* has also been isolated (Yu *et al.* 2015).

519

## 520 **Temperature**

521 The temperatures used here for isolation, cultivation, and tests (Table 5) for both  
522 bacteria and phages were warmer than the temperatures in the sea-ice brine (-1.7  
523 °C down to -12.6 °C; Tison *et al.* 2017), due to methodological limitations. It is  
524 still evident that the bacteria and phages were cold-adapted, since the bacterial  
525 strains were able to grow at 0 °C, but not at 20 °C (Morita 1975), and the phages  
526 were capable of infecting and producing progeny at  $\leq 4$  °C (Wells and Deming  
527 2006b; Table 5). In addition, psychrophilic bacteria from sea ice can be active even  
528 at -20 °C (Junge *et al.* 2004), and cold-active phages can be productive at  
529 temperatures from 8 °C to -6 °C (Wells and Deming 2006b) or even at -12 °C  
530 (Wells and Deming 2006c).

531

532 The phages seemed to retain their infectivity well at cold temperatures, since the  
533 infectivity of the lysates was stable for several months at 4 °C and at -80 °C

1  
2  
3 534 (supplemented with 15% glycerol), consistent with a previous study (Wells and  
4  
5 535 Deming 2006c). Virus plaques were formed only at temperatures about 10 degrees  
6  
7 536 lower than their host could tolerate, indicating that temperature controlled the  
8  
9 537 infections, as shown in previous studies on sea-ice phage-host isolates (Borriss *et*  
10  
11 538 *al.* 2003; Luhtanen *et al.* 2014) and other cold-adapted phage-host systems (Wells  
12  
13 539 and Deming 2006b). The virus-receptor molecules may only have been induced at  
14  
15 540 cold temperatures, as reported previously in *Yersinia enterocolitica* infections  
16  
17 541 (Leon-Velarde *et al.* 2016), indicating that the receptors may be associated with the  
18  
19 542 host's cryoprotection mechanisms. The structure of the phage-receptor molecules  
20  
21 543 could also have changed with rising temperatures, which can inhibit the infection,  
22  
23 544 or the bacterial resistance mechanisms could have been activated at higher  
24  
25 545 temperatures. The phage particles themselves remained infectious and were able to  
26  
27 546 tolerate the temperature of the warm top-layer agar (~43 °C) used for the plaque  
28  
29 547 assay.

30 548

### 31 549 **Abundance of virus-like particles and virus-to-bacteria ratios in Antarctic** 32 33 550 **winter-sea ice**

34  
35 551 The VLP abundance in Antarctic winter-sea ice ranged from  $\sim 10^5$  to  $10^6$  ml<sup>-1</sup> in  
36  
37 552 bulk ice (Table 1). The highest abundances were measured at stations 500 and 515  
38  
39 553 ( $0.7 \times 10^6$ – $4.9 \times 10^6$  ml<sup>-1</sup> in bulk ice). The lower range of our dataset is comparable to  
40  
41 554 the values measured earlier from Antarctic winter-sea ice ( $\sim 10^5$  ml<sup>-1</sup> of bulk ice;  
42  
43 555 Paterson and Laybourn-Parry 2012), whereas the highest abundances were similar  
44  
45 556 to those in Arctic spring blooms and Antarctic late autumn and summer sea ice  
46  
47 557 ( $\sim 10^6$ – $10^8$  ml<sup>-1</sup> of bulk ice; Maranger *et al.* 1994; Gowing *et al.* 2002; 2004,  
48  
49 558 respectively). The high VLP concentrations at stations 500 and 515 may be  
50  
51 559 explained by the high bacterial abundance (Eronen-Rasimus *et al.* 2017; Table 1)  
52  
53 560 and bacterial production (measured as thymidine incorporation; Eronen-Rasimus *et*  
54  
55 561 *al.* 2017) observed, which were positively correlated with the high chl-*a*  
56  
57 562 concentrations (up to 113.2 mg l<sup>-1</sup> in bulk ice; Eronen-Rasimus *et al.* 2017; Tison

1  
2  
3 563 *et al.* 2017). Positive correlation of chl-*a* with bacterial and VLP abundances was  
4 reported in Antarctic sea ice during spring and summer ice-algal blooms  
5 564  
6 565 (Maranger *et al.* 1994; Gowing *et al.* 2004). Our results suggest that if the chl-*a*  
7  
8 566 concentrations and consequent bacterial abundance and activity are high, viruses  
9  
10 567 may be abundant and likely active in winter-sea ice. The high VLPs also indicate  
11  
12 568 that the viral winter-sea-ice community was surprisingly dynamic, considering the  
13  
14 569 season.

15 570

16  
17  
18 571 The VBR range of 0.7–13.4 (mean 5.3) corresponds to those measured previously  
19  
20 572 in Antarctic winter-sea ice (1–20.8; Paterson and Laybourn-Parry 2012). The  
21  
22 573 highest VBRs (Table 1) were found at first-year ice-station 503 with low bacterial  
23  
24 574 abundance and activity (Table 1; see bacterial production in Eronen-Rasimus *et al.*  
25  
26 575 2017), while the lowest VBRs were detected at young second-year ice-station 515  
27  
28 576 (Table 1) with the highest bacterial production and abundance (Eronen-Rasimus *et*  
29  
30 577 *al.* 2017; Table 1). The high VBR in the low-activity community may have  
31  
32 578 resulted from induction of lysogenic viruses during freezing and preservation of  
33  
34 579 the virus particles in sea-ice brine, similarly to young ice in the Arctic (Collins and  
35  
36 580 Deming 2011). The decreasing VBR together with increasing VLP, bacterial  
37  
38 581 abundances, and bacterial activity were also detected during the algal spring bloom  
39  
40 582 (Maranger *et al.* 1994). The low VBR in the active community may have resulted  
41  
42 583 from change in the bacterial community composition, so that the majority of the  
43  
44 584 bacteria could have developed resistance against the phages. Alternatively, the host  
45  
46 585 bacterial activity may have been decreased, which could have lowered the viral  
47  
48 586 production, possibly because the phages may have lysogenized, i.e. become  
49  
50 587 prophages (Maranger *et al.* 1994).

51 588

52 589 In conclusion, four phage-host systems were isolated from both first- and second-  
53  
54 590 year winter-sea ice from the Weddell Sea, Antarctica. The phages seemed to be  
55  
56 591 bacterial strain-specific, but some were able to infect several related bacterial

1  
2  
3 592 strains and one from second-year ice even across classes. The phages were able to  
4  
5 593 retain their infectivity for lengthy periods under cold conditions and infected their  
6  
7 594 host bacteria only in the hosts' lower growth temperature ranges, suggesting that  
8  
9 595 they are cold-active. The VLP counts suggest that the viral community may also be  
10  
11 596 dynamic in winter-sea ice if their hosts are active.

12 597

### 14 598 **Funding**

15  
16 599 This work was supported by the Walter and Andrée de Nottbeck Foundation  
17  
18 600 (AML, EER, JMR), Onni Talas Foundation (AML), the Academy Professor  
19  
20 601 (Academy of Finland) funding grants 283072 and 255342 (DHB) and the Belgian  
21  
22 602 Science Policy (Bigsouth project, SD/CA/05). BD is a research associate at the  
23  
24 603 F.R.S-FNRS.

25 604

### 27 605 **Acknowledgements**

28  
29 606 The authors acknowledge the support and use of resources of Instruct, a Landmark  
30  
31 607 ESFRI project. We thank the University of Helsinki and Academy of Finland  
32  
33 608 (grant number 1306833) for support provided to EU ESFRI Instruct Centre for  
34  
35 609 Virus and Macromolecular Complex Production (ICVIR) used in this study. We  
36  
37 610 also acknowledge the Electron Microscopy Unit in the Institute of Biotechnology,  
38  
39 611 University of Helsinki and the Finnish Environment Institute, Marine Research  
40  
41 612 Centre and Finnish Marine Research Infrastructure (FINMARI) for providing the  
42  
43 613 laboratory infrastructure. We also want to thank the Finnish Antarctic Research  
44  
45 614 Program FINNARP (especially Mika Kalakoski and Eivor Lahtinen) for logistic  
46  
47 615 and financial support with cargo and travel expenses, and the Alfred Wegener  
48  
49 616 Institute for Polar and Marine Research, leading researcher Peter Lemke, the  
50  
51 617 captain, crew, and the other participants in the AW ECS expedition. We thank Sari  
52  
53 618 Korhonen for skilled technical assistance in virus production and purification,  
54  
55 619 Christiane Uhlig for providing the MOX medium plates, and Harri Kuosa and  
56  
57 620 Daniel Delille for useful comments on the manuscript.



621

**Conflict of Interest**

The authors declare no conflict of interest.

624

**References**

Anderson NG, Harris WW, Barber AA *et al.* Separation of subcellular components and viruses by combined rate- and isopycnic-zonal centrifugation. *J Natl Cancer Inst Monogr* 1966;**21**:253–83.

Arrigo KR, Mock T, Lizotte MP. Primary producers and sea ice. In: Thomas DN, Dieckmann GS (eds). *Sea Ice*. 2nd ed. Oxford: John Wiley & Sons, Ltd., 2010, 283–325.

Arrigo KR, Thomas DN. Large scale importance of sea ice biology in the Southern Ocean. *Antarct Sci* 2004;**16**:471–86.

Bamford JK, Bamford DH. Large-scale purification of membrane-containing bacteriophage PRD1 and its subviral particles. *Virology* 1991;**181**:348–52.

Borriss M, Helmke E, Hanschke R *et al.* Isolation and characterization of marine psychrophilic phage-host systems from Arctic sea ice. *Extremophiles* 2003;**7**:377–84.

Borriss M, Lombardot T, Glöckner FO *et al.* Genome and proteome characterization of the psychrophilic *Flavobacterium* bacteriophage 11b. *Extremophiles* 2007;**11**:95–104.

Boulanger PA, Puvion F. Large-scale preparation of soluble adenovirus hexon, penton and fiber antigens in highly purified form. *Eur J Biochem* 1973;**39**:37–42.

Bowman JP, McCammon SA, Brown MV *et al.* Diversity and association of psychrophilic bacteria in Antarctic sea ice. *Appl Environ Microb* 1997;**63**:3068–78.

Bradford MM. A rapid and sensitive method for the quantitation of microgram quantities of protein utilizing the principle of protein-dye binding. *Anal Biochem* 1976;**72**:248–54.

- 1  
2  
3 645 Brinkmeyer R, Knittel K, Jurgens J *et al.* Diversity and structure of bacterial  
4 646 communities in Arctic versus Antarctic pack ice. *Appl Environ Microb* 2003;**69**:6610–9.
- 6  
7 647 Brussaard CPD, Payet JP, Winter C *et al.* Quantification of Aquatic Viruses by Flow  
8 648 Cytometry. In: Wilhelm S, Weinbauer M, Suttle C (eds.). *Manual of Aquatic Viral*  
9 649 *Ecology*. The American society of limnology and Oceanography, Inc, 2010:102–109.
- 12  
13 650 Burgess RR. Chapter 20 - Protein Precipitation Techniques. *Method Enzymol*. Vol 463.  
14 651 1st ed. Elsevier Inc., 2009, 331–42.
- 17  
18 652 Colangelo-Lillis JR, Deming JW. Genomic analysis of cold-active Colwelliophage 9A  
19 653 and psychrophilic phage-host interactions. *Extremophiles* 2013;**17**:99–114.
- 22  
23 654 Collins RE, Deming JW. Abundant dissolved genetic material in Arctic sea ice Part II:  
24 655 Viral dynamics during autumn freeze-up. *Polar Biol* 2011;**34**:1831–41.
- 26  
27 656 Deming JW, Collins RE. Sea ice as a habitat for bacteria, archaea and viruses. In:  
28 657 Thomas DN (ed.). *Sea Ice*. 3rd ed. Oxford: John Wiley & Sons, Ltd., 2017, 326–351.
- 31  
32 658 Dieckmann GS, Hellmer H. The importance of sea ice: an overview. In: Thomas DN,  
33 659 Dieckmann GS (eds). *Sea Ice*. 2nd ed. Oxford: John Wiley & Sons, Ltd., 2010, 1–22.
- 35  
36 660 Edwards U, Rogall T, Blöcker H *et al.* Isolation and direct complete nucleotide  
37 661 determination of entire genes. Characterization of a gene coding for 16S ribosomal  
38 662 RNA. *Nucleic Acids Res* 1989;**17**:7843–53.
- 41  
42 663 Eronen-Rasimus E, Luhtanen A-M, Rintala J-M *et al.* An active bacterial community  
43 664 linked to high chl-a concentrations in Antarctic winter-pack ice and evidence for the  
44 665 development of an anaerobic sea-ice bacterial community. *ISME J* 2017;**63**:3068. DOI:  
45 666 10.1038/ismej.2017.96.
- 49  
50 667 Forterre P, Soler N, Krupovic M *et al.* Fake virus particles generated by fluorescence  
51 668 microscopy. *Trends Microbiol* 2013;**21**:1–5.
- 53  
54  
55  
56  
57  
58  
59  
60

- 1  
2  
3 669 Fuhrman JA. Marine viruses and their biogeochemical and ecological effects. *Nature*  
4 670 1999;**399**:541–8.
- 6  
7 671 Gowing MM, Garrison DL, Gibson AH *et al.* Bacterial and viral abundance in Ross Sea  
8  
9 672 summer pack ice communities. *Mar Ecol Prog Ser* 2004;**279**:3–12.
- 11 673 Gowing MM, Riggs BE, Garrison DL *et al.* Large viruses in Ross Sea late autumn pack  
12 674 ice habitats. *Mar Ecol Prog Ser* 2002;**241**:1–11.
- 15  
16 675 Helmke E, Weyland H. Bacteria in sea ice and underlying water of the eastern Weddell  
17 676 Sea in midwinter. *Mar Ecol Prog Ser* 1995;**117**:269–87.
- 19  
20 677 Huston AL, Krieger-Brockett BB, Deming JW. Remarkably low temperature optima for  
21 678 extracellular enzyme activity from Arctic bacteria and sea ice. *Environ Microbiol*  
22 679 2000;**2**:383–8.
- 25  
26 680 Junge K, Eicken H, Deming JW. Bacterial Activity at -2 to -20 °C in Arctic Wintertime  
27 681 Sea Ice. *Appl Environ Microbiol* 2004;**70**:550–7.
- 29  
30 682 Krupovic M, Dutilh BE, Adriaenssens EM *et al.* Taxonomy of prokaryotic viruses:  
31 683 update from the ICTV bacterial and archaeal viruses subcommittee. *Arch Virol*  
32 684 2016;**161**:1095–9.
- 35  
36 685 Lane DJ, Pace B, Olsen GJ *et al.* Rapid determination of 16S ribosomal RNA sequences  
37 686 for phylogenetic analyses. *Proc Natl Acad Sci* 1985;**82**:6955–9.
- 39  
40 687 Lannuzel D, De Jong J, Schoemann V *et al.* Development of a sampling and flow  
41 688 injection analysis technique for iron determination in the sea ice environment. *Anal Chim*  
42 689 *Acta* 2006;**556**:476–483.
- 45  
46 690 Lawrence JE, Steward GF. Purification of Viruses by Centrifugation. In: Wilhelm S,  
47 691 Weinbauer M, Suttle C (eds.). *Manual of Aquatic Viral Ecology*. The American society  
48 692 of limnology and Oceanography, Inc, 2010:166–181.

- 1  
2  
3 693 Leon-Velarde CG, Happonen L, Pajunen M *et al.* *Yersinia enterocolitica*-specific  
4 694 infection by bacteriophages TG1 and  $\phi$ R1-RT is dependent on temperature-regulated  
5 695 expression of the phage host receptor OmpF. *Appl Environ Microbiol* 2016;**82**:5340–53.
- 6  
7  
8  
9 696 Letunic I, Bork P. Interactive Tree Of Life (iTOL): an online tool for phylogenetic tree  
10 697 display and annotation. *Bioinformatics* 2007;**23**:127–128.
- 11  
12  
13 698 Luhtanen A-M, Eronen-Rasimus E, Kaartokallio H *et al.* Isolation and characterization of  
14 699 phage-host systems from the Baltic Sea ice. *Extremophiles* 2014;**18**:121–30.
- 15  
16  
17  
18 700 Maranger R, Bird DF. Viral abundance in aquatic systems: a comparison between marine  
19 701 and fresh waters. *Mar Ecol Prog Ser* 1995;**121**: 217–226.
- 20  
21  
22 702 Maranger R, Bird D, Juniper S. Viral and bacterial dynamics in Arctic sea ice during the  
23 703 spring algal bloom near Resolute, N. W. T., Canada. *Mar Ecol Prog Ser* 1994;**111**:121–7.
- 24  
25  
26  
27 704 Marchant H, Davidson A, Wright S *et al.* The distribution and abundance of viruses in  
28 705 the Southern Ocean during spring. *Antarct Sci* 2000;**12**:414–7.
- 29  
30  
31 706 Meiners K, Krembs C, Gradinger R. Exopolymer particles: microbial hotspots of  
32 707 enhanced bacterial activity in Arctic fast ice (Chukchi Sea). *Aquat Microb Ecol*  
33 708 2008;**52**:195–207.
- 34  
35  
36  
37 709 Middelboe M, Hagström Å, Blackburn N *et al.* Effects of bacteriophages on the  
38 710 population dynamics of four strains of pelagic marine bacteria. *Microb Ecol*  
39 711 2001;**42**:395–406.
- 40  
41  
42  
43 712 Middelboe M, Riemann L, Steward GF *et al.* Virus-induced transfer of organic carbon  
44 713 between marine bacteria in a model community. *Aquat Microb Ecol* 2003;**33**:1–10.
- 45  
46  
47  
48 714 Mock T, Thomas DN. Recent advances in sea-ice microbiology. *Environ Microbiol*  
49 715 2005;**7**:605–19.
- 50  
51  
52 716 Morita RY. Psychrophilic bacteria. *Bacteriol Rev* 1975;**39**:144–67.
- 53  
54  
55  
56  
57  
58  
59  
60

- 1  
2  
3 717 Olkkonen VM, Bamford DH. Quantitation of the adsorption and penetration stages of  
4 718 bacteriophage  $\phi 6$  infection. *Virology* 1989;**171**:229–238.
- 6  
7 719 Paterson H, Laybourn-Parry J. Antarctic sea ice viral dynamics over an annual cycle.  
8  
9 720 *Polar Biol* 2012;**35**:491–7.
- 11  
12 721 Proctor LM, Fuhrman JA. Viral mortality of marine bacteria and cyanobacteria. *Nature*  
13 722 1990;**343**:60–2.
- 15  
16 723 Pruesse E, Peplies J, Glockner FO. SINA: Accurate high-throughput multiple sequence  
17 724 alignment of ribosomal RNA genes. *Bioinformatics* 2012;**28**:1823–9.
- 19  
20 725 Rintala J-M, Piiparinen J, Blomster J *et al.* Fast direct melting of brackish sea-ice  
21 726 samples results in biologically more accurate results than slow buffered melting. *Polar*  
22 727 *Biol* 2014;**37**:1811–22.
- 24  
25  
26 728 Sait L, Galic M, Strugnell RA *et al.* Secretory Antibodies Do Not Affect the Composition  
27 729 of the Bacterial Microbiota in the Terminal Ileum of 10-Week-Old Mice. *Appl Environ*  
28 730 *Microbiol* 2003;**69**:2100–9.
- 30  
31  
32  
33 731 Senčilo A, Luhtanen A-M, Saarijärvi M *et al.* Cold-active bacteriophages from the Baltic  
34 732 Sea ice have diverse genomes and virus-host interactions. *Environ Microbiol*  
35 733 2015;**17**:3628–41.
- 37  
38  
39 734 Shivaji S, Reddy GS. Phylogenetic analyses of the genus *Glaciecocola*: emended  
40 735 description of the genus *Glaciecocola*, transfer of *Glaciecocola mesophila*, *G. agarilytica*, *G.*  
41 736 *aquimarina*, *G. arctica*, *G. chathamensis*, *G. polaris* and *G. psychrophila* to the genus  
42 737 *Paraglaciecola* gen. nov. as *Paraglaciecola mesophila* comb. nov., *P. agarilytica* comb.  
43 738 nov., *P. aquimarina* comb. nov., *P. arctica* comb. nov., *P. chathamensis* comb. nov., *P.*  
44 739 *polaris* comb. nov. and *P. psychrophila* comb. nov., and description of *Paraglaciecola*  
45 740 *oceanifecundans* sp. nov., isolated from the Southern Ocean. *Inter J Syst Evol Micr*  
46 741 2014;**64**:3264–75.
- 48  
49  
50  
51  
52  
53  
54 742 Soler N, Krupovic M, Marguet E *et al.* Membrane vesicles in natural environments: a  
55 743 major challenge in viral ecology. *ISME J* 2015;**9**:793–6.

- 1  
2  
3 744 Stamatakis A. RaxML version 8: a tool for phylogenetic analysis and post-analysis of  
4 745 large phylogenies. *Bioinformatics* 2014;**30**:1312–1313.
- 6  
7 746 Suttle C. Viruses in the sea. *Nature* 2005;**437**:356–61.
- 9  
10 747 Suttle CA. Marine viruses – major players in the global ecosystem. *Nat Rev Micro*  
11 748 2007;**5**:801–12.
- 13  
14 749 Thingstad T, Lignell R. Theoretical models for the control of bacterial growth rate,  
15 750 abundance, diversity and carbon demand. *Aquat Microb Ecol* 1997;**13**:19–27.
- 18  
19 751 Thingstad TF, Vage S, Storesund JE *et al.* A theoretical analysis of how strain-specific  
20 752 viruses can control microbial species diversity. *Proc Natl Acad Sci USA* 2014;**111**:7813–  
21 753 8.
- 24  
25 754 Thomas DN, Dieckmann GS. Antarctic sea ice – a habitat for extremophiles. *Science*  
26 755 2002;**295**:641–4.
- 28  
29 756 Tison J-L, Schwegmann S, Dieckmann G *et al.* Biogeochemical impact of snow cover  
30 757 and cyclonic intrusions on the winter Weddell Sea ice pack. *J Geophys Res Oceans* 2017.  
31 758 DOI: 10.1002/2017jc013288.
- 34  
35 759 Weinbauer MG. Ecology of prokaryotic viruses. *FEMS Microbiol Rev* 2004;**28**:127–81.
- 37  
38 760 Wells L, Deming J. Modelled and measured dynamics of viruses in Arctic winter sea-ice  
39 761 brines. *Environ Microbiol* 2006a;**8**:1115–21.
- 41  
42  
43 762 Wells LE, Deming JW. Characterization of a cold-active bacteriophage on two  
44 763 psychrophilic marine hosts. *Aquat Microb Ecol* 2006b;**45**:15–29.
- 46  
47 764 Wells LE, Deming JW. Effects of temperature, salinity and clay particles on inactivation  
48 765 and decay of cold-active marine Bacteriophage 9A. *Aquat Microb Ecol* 2006c;**45**:31–9.
- 50  
51 766 Wommack KE, Colwell RR. Virioplankton: Viruses in Aquatic Ecosystems. *Microbiol*  
52 767 *Mol Biol R* 2000;**64**:69–114.

- 1  
2  
3 768 Yoon SH, Ha S-M, Kwon S *et al.* Introducing EzBioCloud: a taxonomically united  
4 769 database of 16S rRNA gene sequences and whole-genome assemblies. *Int J Syst Evol*  
5 770 *Microbiol* 2017;**67**:1613–1617.
- 6  
7  
8  
9 771 Yu Z-C, Chen X-L, Shen Q-T *et al.* Filamentous phages prevalent in *Pseudoalteromonas*  
10 772 spp. confer properties advantageous to host survival in Arctic sea ice. *ISME J*  
11 773 2015;**9**:871–81.
- 12  
13  
14  
15  
16  
17  
18  
19  
20  
21  
22  
23  
24  
25  
26  
27  
28  
29  
30  
31  
32  
33  
34  
35  
36  
37  
38  
39  
40  
41  
42  
43  
44  
45  
46  
47  
48  
49  
50  
51  
52  
53  
54  
55  
56  
57  
58  
59  
60

For Peer Review

1  
2  
3  
4  
5  
6  
7  
8  
9  
10  
11  
12  
13  
14  
15  
16  
17  
18  
19  
20  
21  
22  
23  
24  
25  
26  
27  
28  
29  
30  
31  
32  
33  
34  
35  
36  
37  
38  
39  
40  
41  
42  
43  
44  
45  
46  
47  
48  
49  
50  
51  
52  
53  
54  
55  
56  
57  
58  
59  
60

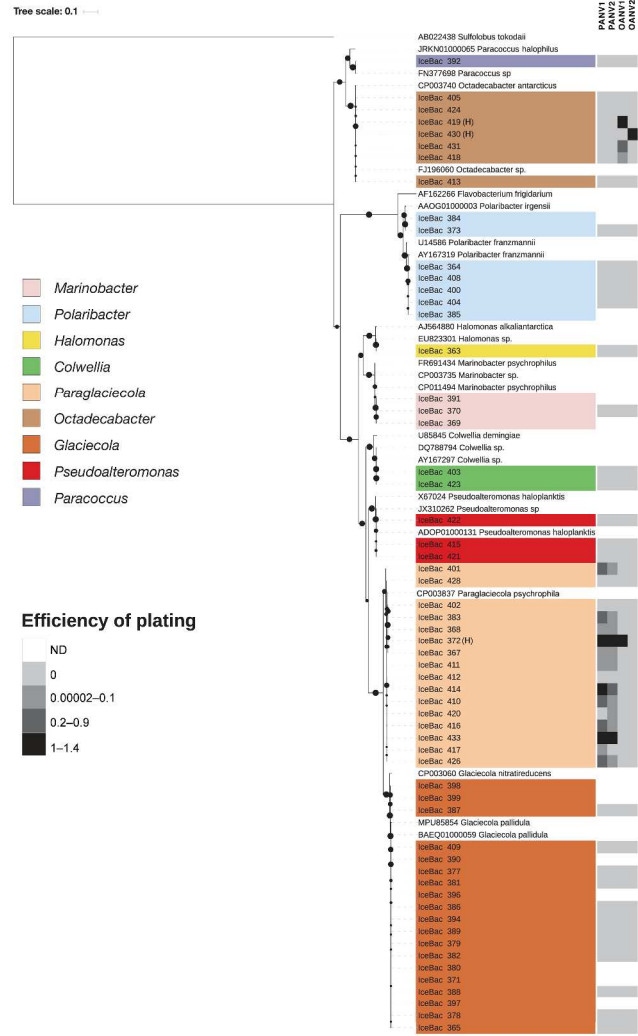


Figure 1 Bootstrapped (1000) phylogenetic maximum-likelihood tree of the 16S rRNA gene sequences of the bacterial strains isolated from Antarctic sea ice. The bootstrap values (> 50%) are shown with black circles. The *Sulfolobus tokodaii* sequence (AB022438) was used as an outgroup in the alignment. The strains are colored at the genus level (see the color key), based on their classification with SILVA Incremental Aligner (SINA) (version 1.2.11, minimum identity: 0.8, Pruesse et al., 2012). The sensitivities of the bacterial strains to isolated phages are shown as efficiency of plating (EOP; on right in gray scale). For the original host (marked by H), the EOP was set to a value of 1. The strains used as references or that do not form a lawn on solid growth media were not tested for EOP (marked with white). The scale bar indicates nucleotide substitutions per position.

421x620mm (600 x 600 DPI)



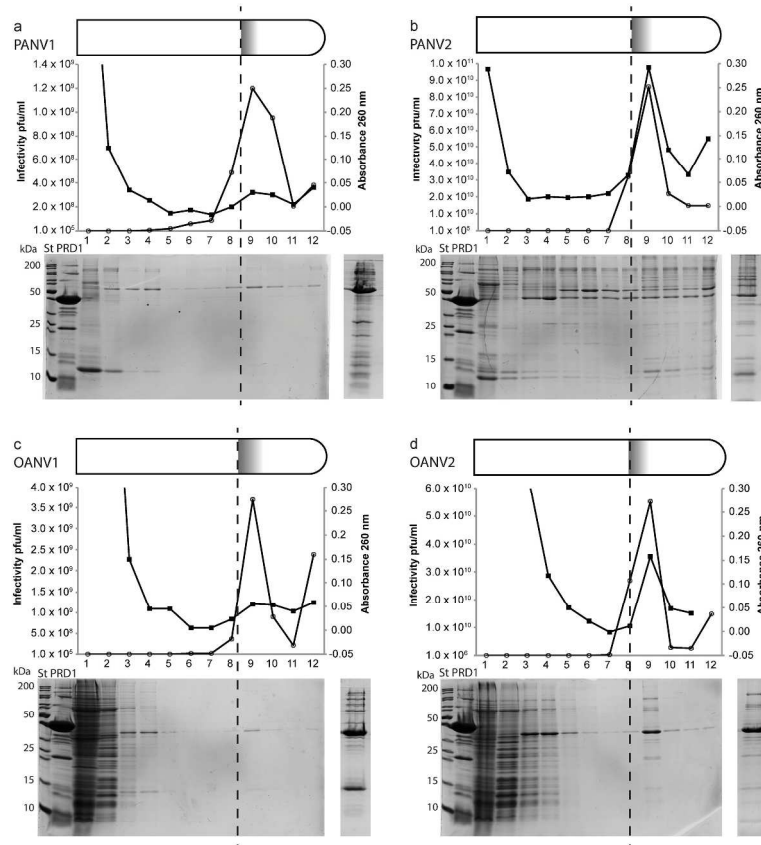
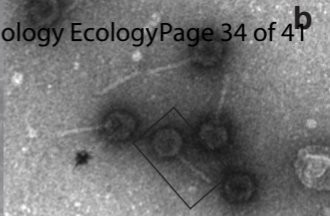
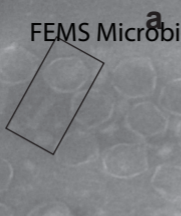


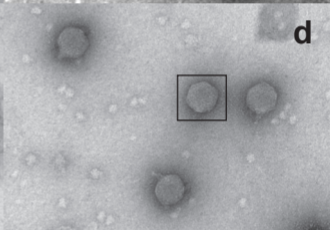
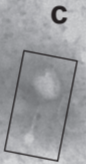
Figure 2 Purification of the phages by rate-zonal centrifugation in sucrose. (a) bacteriophage PANV1, (b) bacteriophage PANV2, (c) bacteriophage OANV1, (d) bacteriophage OANV2. (a–d) Top: position of the light-scattering zone (gray) in the sucrose gradient tubes. Middle: Absorbance (closed squares) and infectivity (open circles) of the 12 sucrose gradient fractions in which the top fraction is marked as 1. Bottom: Protein content of the 12 gradient fractions analyzed with SDS-PAGE and Coomassie Blue staining. The protein patterns of the final biochemically purified and concentrated phages are shown on the right. St = molecular mass marker; PRD1 = purified phage PRD1 used as a control. The dashed line marks the position of the upper edge of the light-scattering virus zone. pfu = plaque-forming unit.

279x373mm (300 x 300 DPI)

1  
2  
3  
4  
5  
6  
7  
8  
9



**10** 100 nm



11  
12  
13  
14  
15  
16  
17

1  
2  
3  
4  
5  
6  
7  
8  
9  
10  
11  
12  
13  
14  
15  
16  
17  
18  
19  
20  
21  
22  
23  
24  
25  
26  
27  
28  
29  
30  
31  
32  
33  
34  
35  
36  
37  
38  
39  
40  
41  
42  
43  
44  
45  
46  
47  
48  
49  
50  
51  
52  
53  
54  
55  
56  
57  
58  
59  
60

## Figure legends

**Figure 1** Bootstrapped (1000) phylogenetic maximum-likelihood tree of the 16S rRNA gene sequences of the bacterial strains isolated from Antarctic sea ice. The bootstrap values (> 50%) are shown with black circles. The *Sulfolobus tokodaii* sequence (AB022438) was used as an outgroup in the alignment. The strains are colored at the genus level (see the color key), based on their classification with SILVA Incremental Aligner (SINA) (version 1.2.11, minimum identity: 0.8, Pruesse *et al.*, 2012). The sensitivities of the bacterial strains to isolated phages are shown as efficiency of plating (EOP; on right in gray scale). For the original host (marked by H), the EOP was set to a value of 1. The strains used as references or that do not form a lawn on solid growth media were not tested for EOP (marked with white). The scale bar indicates nucleotide substitutions per position.

**Figure 2** Purification of the phages by rate-zonal centrifugation in sucrose. **(a)** bacteriophage PANV1, **(b)** bacteriophage PANV2, **(c)** bacteriophage OANV1, **(d)** bacteriophage OANV2. **(a-d) Top:** position of the light-scattering zone (gray) in the sucrose gradient tubes. **Middle:** Absorbance (closed squares) and infectivity (open circles) of the 12 sucrose gradient fractions in which the top fraction is marked as 1. **Bottom:** Protein content of the 12 gradient fractions analyzed with SDS-PAGE and Coomassie Blue staining. The protein patterns of the final biochemically purified and concentrated phages are shown on the right. St = molecular mass marker; PRD1 = purified phage PRD1 used as a control. The dashed line marks the position of the upper edge of the light-scattering virus zone. pfu = plaque-forming unit.

**Figure 3** Transmission electron micrographs of the purified and negatively stained phages. **(a)** PANV1, **(b)** PANV2, **(c)** OANV1, and **(d)** OANV2.

Table 1. VLP and bacterial abundances and virus-to-bacteria ratios (VBRs) in the different layers of ice cores from all the AWECS sampling stations.

Station	Date	Latitude	Longitude	Ice depth (cm) from air-ice interface		VLP x 10 <sup>5</sup> /ml in bulk ice <sup>b</sup>	Bacteria x 10 <sup>5</sup> /ml in bulk ice <sup>b,c</sup>	VBR VLP/Bacteria
				Core I	Core II			
486 <sup>a</sup>	6/17/2013	-61.526	-0.086	0–6	–	1.90	0.56	3.4
488 <sup>a</sup>	6/18/2013	-62.928	-0.006	0–15	–	4.90	0.56	8.8
				15–20	–	2.60	0.81	3.2
				20–35	–	6.80	1.20	5.7
489 <sup>a</sup>	6/19/2013	-63.901	-0.031	0–15	–	6.50	1.20	5.4
				15–22	–	4.90	1.30	3.8
				22–37	–	5.80	0.85	6.8
493	6/21/2013	-66.44	0.122	0–15	0–15	13.00	3.40	3.8
				15–46	15–38	9.30	3.80	2.4
				46–61	38–53	9.30	1.80	5.2
496	6/24/2013	-67.466	-0.021	0–15	0–15	4.70	1.30	3.6
				15–45	15–57	3.90	2.70	1.4
				45–60	57–72	5.90	2.50	2.4
500	7/3/2013	-67.949	-6.658	0–15	0–15	16.00	2.60	6.2
				15–35	15–35	12.00	3.60	3.3
				35–55	35–52	46.00	4.00	11.5
				55–75	52–72	20.00	3.40	5.9
				75–90	72–87	9.70	2.70	3.6
503	7/8/2013	-67.187	-13.224	0–15	0–15	8.70	0.65	13.4
				15–25	15–25	7.50	0.79	9.5
				25–37	25–36	9.20	0.81	11.4
				37–47	36–46	10.00	0.80	12.5
				47–62	46–61	6.70	0.56	12.0
506	7/11/2013	-67.19	-23.042	0–15	0–15	3.90	0.51	7.6
				15–34	15–30	5.50	0.80	6.9
				34–49	30–45	ND	ND	ND
515 <sup>a</sup>	7/26/2013	-63.456	-51.308	0–15	–	6.90	3.60	1.9
				15–45	–	9.30	6.00	1.6
				45–75	–	21.00	7.30	2.9
				75–104	–	40.00	24.00	1.7
				104–134	–	49.00	42.00	1.2
				134–164	–	10.00	9.50	1.1
517	7/30/2013	-63.509	-51.112	0–15	0–15	5.70	0.60	9.5
				15–30	15–30	4.60	0.87	5.3
				30–43	30–43	2.20	0.71	3.1
				43–58	43–58	2.40	1.30	1.8
				58–73	58–73	5.80	1.40	4.1

<sup>a</sup> Only one ice core sampled

<sup>b</sup> Analysed from combined layers of the sibling cores I and II, when two cores were collected.

<sup>c</sup> Bacterial abundances are also published in Eronen-Rasmus et al. (2017)

VLP = virus-like particle, AWECS = Antarctic Winter Ecosystem Climate Study, ND = not determined

Table 2. Bacterial strains isolated in this study from the ice core 515a.

Isolation depth from air-ice interface (cm)	Isolation media <sup>a</sup>	Bacterial strain	Closest match genus <sup>b</sup>	Identity % at genus level	Accession number	Used for virus isolation
0-14	Z	IceBac 363	<i>Halomonas</i>	100.0	KY194856	✓
14-28	Z	IceBac 364	<i>Polaribacter</i>	99.7	KY194850	✓
14-28	Z	IceBac 365	<i>Glaciecola</i>	99.6	KY194821	✓
14-28	Z	IceBac 367	<i>Paraglaciecola</i>	99.9	KY194799	✓
14-28	Z	IceBac 368	<i>Paraglaciecola</i>	99.9	KY194805	✓
14-28	Z	IceBac 369	<i>Marinobacter</i>	99.3	KY194841	
14-28	Z	IceBac 370	<i>Marinobacter</i>	99.3	KY194842	✓
14-28	Z	IceBac 371	<i>Glaciecola</i>	99.6	KY194822	
14-28	Z	IceBac 372	<i>Paraglaciecola (H)</i>	99.9	KY194800	✓
14-28	MOX	IceBac 373	<i>Polaribacter</i>	100.0	KY194848	✓
14-28	MOX	IceBac 377	<i>Glaciecola</i>	99.6	KY194823	✓
28-42	Z	IceBac 378	<i>Glaciecola</i>	99.6	KY194828	✓
28-42	Z	IceBac 379	<i>Glaciecola</i>	99.6	KY194824	✓
28-42	Z	IceBac 380	<i>Glaciecola</i>	99.6	KY194825	
28-42	Z	IceBac 381	<i>Glaciecola</i>	99.6	KY194829	✓
28-42	Z	IceBac 382	<i>Glaciecola</i>	99.6	KY194831	✓
28-42	Z	IceBac 383	<i>Paraglaciecola</i>	99.9	KY194801	✓
28-42	MOX	IceBac 384	<i>Polaribacter</i>	100.0	KY194845	
42-56	Z	IceBac 385	<i>Polaribacter</i>	99.7	KY194844	
42-56	Z	IceBac 386	<i>Glaciecola</i>	99.6	KY194815	✓
42-56	Z	IceBac 387	<i>Glaciecola</i>	99.5	KY194816	✓
42-56	Z	IceBac 388	<i>Glaciecola</i>	99.6	KY194826	✓
42-56	Z	IceBac 389	<i>Glaciecola</i>	99.6	KY194817	✓
42-56	Z	IceBac 390	<i>Glaciecola</i>	99.6	KY194830	
42-56	Z	IceBac 391	<i>Marinobacter</i>	99.3	KY194843	
42-56	Z	IceBac 392	<i>Paracoccus</i>	99.9	KY194857	✓
42-56	MOX	IceBac 394	<i>Glaciecola</i>	99.6	KY194832	✓
56-70	Z	IceBac 396	<i>Glaciecola</i>	99.6	KY194827	
56-70	Z	IceBac 397	<i>Glaciecola</i>	99.6	KY194818	
56-70	Z	IceBac 398	<i>Glaciecola</i>	99.5	KY194820	
56-70	Z	IceBac 399	<i>Glaciecola</i>	99.4	KY194819	
56-70	Z	IceBac 400	<i>Polaribacter</i>	99.7	KY194849	✓
56-70	Z	IceBac 401	<i>Paraglaciecola</i>	100.0	KY194802	✓
56-70	Z	IceBac 402	<i>Paraglaciecola</i>	99.9	KY194806	✓
70-84	C	IceBac 403	<i>Colwellia</i>	99.4	KY194851	✓
70-84	Z	IceBac 404	<i>Polaribacter</i>	99.7	KY194846	✓
70-84	Z	IceBac 405	<i>Octadecabacter</i>	100.0	KY194834	✓
98-112	Z	IceBac 408	<i>Polaribacter</i>	99.7	KY194847	✓
98-112	Z	IceBac 409	<i>Glaciecola</i>	99.6	KY194833	✓

112-126	C	IceBac 410	<i>Paraglaciecola</i>	100.0	KY194813	✓
112-126	Z	IceBac 411	<i>Paraglaciecola</i>	100.0	KY194808	✓
112-126	Z	IceBac 412	<i>Paraglaciecola</i>	100.0	KY194803	✓
112-126	Z	IceBac 413	<i>Octadecabacter</i>	100.0	KY194835	✓
112-126	Z	IceBac 414	<i>Paraglaciecola</i>	100.0	KY194804	✓
126-140	C	IceBac 415	<i>Pseudoalteromonas</i>	100.0	KY194855	✓
126-140	Z	IceBac 416	<i>Paraglaciecola</i>	99.9	KY194807	✓
126-140	Z	IceBac 417	<i>Paraglaciecola</i>	100.0	KY194809	✓
126-140	Z	IceBac 418	<i>Octadecabacter</i>	100.0	KY194836	✓
126-140	Z	IceBac 419	<i>Octadecabacter (H)</i>	100.0	KY194837	✓
140-154	Z	IceBac 420	<i>Paraglaciecola</i>	100.0	KY194810	✓
140-154	Z	IceBac 421	<i>Pseudoalteromonas</i>	100.0	KY194853	✓
140-154	Z	IceBac 422	<i>Pseudoalteromonas</i>	100.0	KY194854	✓
140-154	Z	IceBac 423	<i>Colwellia</i>	99.4	KY194852	✓
140-154	Z	IceBac 424	<i>Octadecabacter</i>	100.0	KY194838	✓
140-154	MOX	IceBac 426	<i>Paraglaciecola</i>	100.0	KY194814	✓
154-166	Z	IceBac 428	<i>Paraglaciecola</i>	99.9	KY194811	✓
154-166	Z	IceBac 430	<i>Octadecabacter (H)</i>	100.0	KY194839	✓
154-166	Z	IceBac 431	<i>Octadecabacter</i>	100.0	KY194840	✓
154-166	MOX	IceBac 433	<i>Paraglaciecola</i>	100.0	KY194812	✓

<sup>a</sup> Z = Zobell media; MOX= MOX media; C = concentrated Zobell media.

<sup>b</sup> Original isolation hosts of the viruses are marked by (H).

1  
2  
3  
4  
5  
6  
7  
8  
9  
10  
11  
12  
13  
14  
15  
16  
17  
18  
19  
20  
21  
22  
23  
24  
25  
26  
27  
28  
29  
30  
31  
32  
33  
34  
35  
36  
37  
38  
39  
40  
41  
42  
43  
44  
45  
46  
47

**Table 3.** Phages isolated in this study.

Phage	Sampling station	Isolation host	Genus of the host (closest match)	Lysate titer (pfu/ml)	Capsid head diameter (nm) <sup>a</sup>	Tail length (nm) <sup>b</sup>	Morphotype
<i>Paraglaciecola</i> Antarctic GD virus 1 (PANV1)	500	IceBac 372	<i>Paraglaciecola</i>	$1.5 \times 10^{10}$	71±7 (n=20)	58±22 (n=10)	myovirus
<i>Paraglaciecola</i> Antarctic JLT virus 2 (PANV2)	500	IceBac 372	<i>Paraglaciecola</i>	$5.2 \times 10^{11}$	52±8 (n=29)	89±30 (n=10)	siphovirus
<i>Octadecabacter</i> Antarctic BD virus 1 (OANV1)	515	IceBac 419	<i>Octadecabacter</i>	$1.2 \times 10^{10}$	50±8 (n=20)	83±10 (n=10)	siphovirus
<i>Octadecabacter</i> Antarctic DB virus 2 (OANV2)	515	IceBac 430	<i>Octadecabacter</i>	$5.8 \times 10^9$	53±7 (n=20)	–	podovirus

<sup>a</sup> average diameter  
<sup>b</sup> average length  
 pfu = plaque-forming unit

For Peer Review

**Table 4.** Recovery of infectious phages during biochemical purification after ammonium sulfate precipitation and rate zonal centrifugation in sucrose combined with concentration step by differential centrifugation.

		Total pfus <sup>a</sup>	Recovery of infectivity %	Specific infectivity pfu / mg protein
<b>PANV1</b>				
	Virus lysate	$7.5 \times 10^{12}$	100.0	
	50 % ammonium sulfate precipitate	$4.1 \times 10^{12}$	54.7	
	Concentrated virus <sup>b</sup>	$1.5 \times 10^{12}$	20.0	$1.8 \times 10^{12}$
<b>PANV2</b>				
	Virus lysate	$3.2 \times 10^{14}$	100.0	
	50 % ammonium sulfate precipitate	$9.6 \times 10^{13}$	30.0	
	Concentrated virus <sup>b</sup>	$6.2 \times 10^{13}$	19.4	$8.9 \times 10^{12}$
<b>OANV1</b>				
	Virus lysate	$6.0 \times 10^{12}$	100.0	
	80 % ammonium sulfate precipitate	$1.5 \times 10^{12}$	25.0	
	Concentrated virus <sup>b</sup>	$5.7 \times 10^{11}$	9.5	$3.8 \times 10^{12}$
<b>OANV2</b>				
	Virus lysate	$3.3 \times 10^{12}$	100.0	
	80 % ammonium sulfate precipitate	$1.2 \times 10^{12}$	35.7	
	Concentrated virus <sup>b</sup>	$4.4 \times 10^{11}$	13.6	$6.9 \times 10^{12}$

<sup>a</sup> calculated per a liter of original lysate

<sup>b</sup> after rate zonal centrifugation in sucrose and concentration by differential centrifugation  
pfu = plaque-forming unit



**Table 5.** Temperature-dependent growth of the bacterial host strains and the phages.

Host bacterial growth <sup>a</sup>					
	<b>0°</b>	<b>4°</b>	<b>10°</b>	<b>15°</b>	<b>20°</b>
IceBac 372	+	+	+	(+)	-
IceBac 419	+	+	+	+	-
IceBac 430	+	+	+	+	-
Infectivity of the phages <sup>a</sup>					
PANV1	+	+	-	-	ND
PANV2	+	+	-	-	ND
OANV1	+	+	-	-	ND
OANV2	+	+	-	-	ND

<sup>a</sup> + = producing colonies/plaques; (+) = retarded growth; - = no colonies or plaques produced; ND = not determined.